

***In silico* Evaluation of the Potential of Natural Products from Chili Pepper as Antiviral Agents Against Dna-Directed Rna Polymerase of the Monkeypox Virus**

Özkan FİDAN^{1*}, Somdutt MUJWAR²

¹Department of Bioengineering, Faculty of Life and Natural Sciences, Abdullah Gül University, Kayseri, Türkiye, 38080

²Chitkara College of Pharmacy, Chitkara University, Rajpura-140401 Punjab, India



(ORCID: [0000-0001-5312-4742](https://orcid.org/0000-0001-5312-4742)) (ORCID: [0000-0003-4037-5475](https://orcid.org/0000-0003-4037-5475))

Keywords: Antiviral agents, Alpha-amyrin, Chili pepper, Monkeypox virus, Virtual screening.

Abstract

This study focused on the discovery of new drug candidates effective against the monkeypox virus. Virtual screening was performed to evaluate the potential of chili pepper natural products against homology-modeled DNA-directed RNA polymerase of the monkeypox virus using molecular docking. Our findings revealed that structurally similar triterpenes such as α -amyrin, β -amyrin, and β -sitosterol had strong binding affinities towards the DNA-directed RNA polymerase and can inhibit this pivotal viral enzyme. The stability of one of the drug candidate molecules, α -amyrin with the strongest binding affinity towards the binding cavity of the enzyme was also confirmed via molecular dynamics simulation. This study showed that α -amyrin is a promising DNA-directed RNA polymerase inhibitor to treat monkeypox disease. It also paves the way for the idea of the potential dietary supplement candidate for monkeypox patients.

1. Introduction

Human monkeypox is a zoonotic disease caused by monkeypox virus. Its clinical manifestations such as fever and skin lesions are similar to smallpox disease, which devastated the humankind in the history and identified as a potential bioterrorism agent [1, 2]. Since then, mostly African countries have been affected with the monkeypox outbreaks. Nevertheless, there have also been cases reported from other countries. Indeed, it has become a public health concern over the globe [3]. Generally, two different clades of monkeypox have been described as Central African clade with the fatality rate of ~10% and West African clade with the fatality rate of ~3% [4, 5].

According to WHO, the main mode of transmission of monkeypox virus takes place from animal to

human due to direct contact with infected animals and handling their raw meat. In fact, it can also be transmitted from human to human through respiratory droplets, direct contact with body fluids, sexual intercourse, and transplacental transfer. The infection has two periods; the first one is the incubation period during which fever, intense headache, lymphadenopathy, back pain, myalgia and intense asthenia are observed. Particularly, lymphadenopathy, which is the swelling of the lymph nodes, is a distinctive symptom of monkeypox disease as compared to similar diseases such as chickenpox and smallpox. In the second period, skin eruption is observed and the rash is more likely to be mostly seen on the face and extremities more than on the trunk.

Monkeypox virus is a double-stranded DNA virus with the genome size of about 197 kbp, which exhibits around 96% identity to the smallpox virus [6, 7]. It is

*Corresponding author: ozkan.fidan@agu.edu.tr

Received: 09.11.2023, Accepted: 09.02.2024

a member of poxviruses that belong to the orthopoxvirus genus including the closely related variola, monkeypox, cowpox, and vaccinia viruses. Studies indicated that monkeypox virus is more closely related to variola than to vaccinia virus [7, 8]. Monkeypox virus cases have recently been reported in UK on 13 May 2022. Since then, multiple cases of monkeypox were reported in several non-endemic countries including the US and other European countries. They were identified as Western African clade [3, 9]. According to Centers for Disease Control and Prevention (CDC), as of 1 of November 2023, the number of monkeypox cases in the US approached to almost 31,000 confirmed cases and the total number of cases reached to more than 91,000 over the world. For this outbreak, the rate of transmission is relatively high compared to previous outbreaks and it is suspected to be due to mutations enhancing human transmission. A significant portion of cases has been reported due to sexually transmitted infections with a perianal or genital rash, which were observed among men who have sex with men [3, 10, 11].

For the treatment of monkeypox, there are no effective drugs currently available in the medicine. However, brincidofovir and tecovirimat are approved by FDA for the treatment smallpox, which is due to a potential biowarfare with smallpox [12, 13]. In animal models, these two drug molecules have also been effective against orthopoxviruses including monkeypox [14, 15]. In a recent case study in UK, out of seven monkeypox patients, three of them were orally treated with brincidofovir and one received tecovirimat, while the remaining patients were not treated with any antiviral drug. In patients treated with brincidofovir, elevated liver enzymes was observed and the therapy was ended, while for the patients treated with tecovirimat, no adverse effects were seen. This case study revealed that it is urgent to conduct the future prospective studies of these antivirals for monkeypox disease treatment [16]. With the current knowledge, a definitive conclusion cannot be drawn for these drugs to be used in the treatment of monkeypox disease [10, 17].

As WHO declared monkeypox as a global health emergency and the unavailability of approved drugs for the treatment of monkeypox, the discovery and development of new drug candidates become increasingly important. Therefore, in this study, we investigated the potential of natural products from chili pepper against monkeypox virus using *in silico* approaches. Particularly, natural products from chili pepper were docked against homology-modeled DNA-directed RNA polymerase. The articles in the literature about the chemical composition of chili pepper was used to prepare the list of chili pepper natural products including capsaicinoids, carotenoids,

terpenoids, flavonoids. In specific, capsaicinoids occupy the majority of the natural product composition [18, 19]. RNA polymerases have been used as an important drug target for various viruses such as SARS-CoV-2, hepatitis C virus, cowpox virus, Zika virus, influenza viruses, and so on [20–23]. Chili extracts and one of the important constituent, capsaicin, were previously tested against some viral species including herpes simplex virus, Lassa virus, and SARS-CoV-2 [24–27]. The results clearly indicated the high potential of chili pepper natural products as antiviral agents. Considering the dietary supplement potential of chili pepper natural products, the discovery of the drug or dietary supplement candidate/s from chili pepper can extend the options for the treatment of monkeypox disease. Our docking results showed α -amyrin has the strongest affinity for DNA-directed RNA polymerase of monkeypox virus. This result was further confirmed in molecular dynamics simulations during which α -amyrin stably bound to DNA-directed RNA polymerase of monkeypox virus throughout the simulation. Thus, our study reveals that α -amyrin is a potential DNA-directed RNA polymerase inhibitor to treat monkeypox disease. It also puts forth the idea of the potential dietary supplement candidate for monkeypox patients.

2. Materials and Methods

2.1. Design and Preparation of Ligand Library

A ligand library from chili pepper, *Capsicum annum*, was created by exploring the literatures from various sources. 47 ligands were shortlisted for generating a ligand library. Their two-dimensional structures were obtained in isomeric SMILES from PubChem Database and subsequently converted into three-dimensional structures through energy minimization process in ChemDraw 8.0 software. All the ligands with three-dimensional structure were eventually prepared for molecular docking experiment using AutoDock Tools software, in which aromatic carbon and rotatable bonds were detected, torsion number was automatically set, non-polar hydrogens were merged, and Gasteiger charges were added for all ligand molecules [22].

2.2. Homology Modeling

DNA-directed RNA polymerase is the main physiological enzyme of monkey-pox virus and is involved in the catalysis of the viral transcription process to form RNA from DNA by utilizing the nucleotides [28–30]. DNA-directed RNA polymerase is essential for regulating the important process of

viral transcription for the synthesis of viral RNA, which is further required by the virus to biosynthesize the various structural and functional proteins. The unavailability of the three-dimensional structural model of this enzyme led us to developing a structural model by using homology modeling approach. The protein sequence of the DNA-directed RNA polymerase of monkeypox virus required for performing homology modeling was obtained from Uniprot database (Sequence ID: Q8V4V3) by using Swiss-Modeller webserver [29, 31]. The modeled macromolecular structure was validated by using Ramachandran plot [32]. Ramachandran plot depicts the position of amino acids in the 'favorable' or 'disallowed' regions based upon the analysis of the torsional phi and psi angles of the macromolecular backbone.

2.3. Molecular Docking Studies

Three-dimensional structure model of the DNA-directed RNA polymerase prepared by homology modeling was used to proceed further with molecular docking studies. Macromolecular structure of the target protein was prepared for molecular docking simulation studies by assigning autodock atom type, Gasteiger charge and its equal distribution among the macromolecular residues [33]. The utilized docking protocol was internally validated by docking the structural model of the target protein with an endogenous ligand, S-adenosylmethionine (SAM). After the validation of the docking protocol, the similar parameters were further utilized for computational screening of the ligand library against the macromolecular drug target protein used in the current study [22, 34].

2.4. Pharmacokinetic and Toxicological Evaluation

The lead molecule must possess qualities that will enable it to be therapeutically effective within the body. Therefore, assessing the ADME characteristics (absorption, distribution, metabolism, and excretion) of the chemical is a significant part of the drug development process. Computer simulations can be a suitable substitute for biological studies in predicting the pharmacokinetic profile of new ligands, leading to higher success rate, lower costs, and a decrease in the number of animals used for experimental testing. The pkCSM-pharmacokinetics server was employed to anticipate the physicochemical, pharmacokinetic, and toxicological characteristics of the lead compound identified from the docking-based screening [35–37]. Major pharmacokinetic characteristics, such as blood-brain barrier (BBB) permeability and passive human

gastrointestinal absorption (HIA), may be easily estimated using pkCSM. Molecular weight (MW), topological polar surface area (TPSA), partition coefficient (LogP), rotatable bonds count, hydrogen bond acceptor/donor (HBA/HBD), and solubility (LogS) of the lead compounds were calculated. These variables control the lead candidates' ADME-T profile. The druggability of lead molecules was further determined by their gastrointestinal absorption, permeability across BBB, and the inhibitory potential of the cytochrome P450 isoenzymes [37–39]. Lipinski's rules of five, Veber's rule, and druggability were used to standardize these characteristics. pkCSM permits substances to be tested for cytochrome P450 (CYP) inhibitory action. This is an essential topic since CYP isoforms are engaged in medication excretion via metabolic biotransformation, affecting therapeutic efficiency as well as drug toxicity and side effects [37, 40].

2.5. Molecular Dynamics Simulation

The Desmond program of Schrödinger was utilized to execute MD simulations for 100 ns on the macromolecular complex of α -amyrin and a homology-modeled viral DNA-directed RNA polymerase, which were acquired from the virtual screening, to further investigate their binding strength and binding pattern [38, 39]. The TIP3P explicit water model was employed to create a simulation box with an orthorhombic shape and a 10 Å gap between the ligand-protein complex and the wall of the box. To establish an isosmotic environment, counter ions were added to neutralize the charge, with a concentration of 0.15 M NaCl. The system was optimized by carrying out 2000 iterations with a merging criterion of 1 kcal/mol. MD simulations were then conducted with the minimized energy complex system. The temperature and air pressure were monitored, with 300K and 1.013 bars respectively, for the duration of the simulation. The trajectory path was adjusted to 9.6 and the energy interval was changed to 1.2 ps, with the resulting trajectories being used to generate simulation interaction diagrams at the end of the simulation [33, 34, 40].

3. Results and Discussion

3.1. Homology Modeling

The protein sequence of viral target protein DNA-directed RNA polymerase obtained from UniProt database consists of 1750 amino acid residues. The homology modeling of this protein sequence was performed by using crystallized structure model of DNA-dependent RNA polymerase subunit rpo132 from vaccinia virus (PDB ID: 6RID) and poxvirus (PDB ID: 7AMV) with the help of SWISS-MODEL webserver [41, 42]. The validation of the prepared structural model of viral DNA-dependent RNA polymerase was performed using a Ramachandran plot. The Ramachandran plot obtained for the structural model of DNA-directed RNA polymerase of monkeypox virus revealed that the structural model has 97.519% residues observed in the highly preferred region demonstrated in green colour, 2.195% residues were in the preferred region demonstrated in orange colour, while 0.286% residues were observed in the non-preferred region demonstrated in red colour (Figure 1).

3.2. Molecular Docking Studies

The three-dimensional structural model of the macromolecular target protein used in this study was tested against SAM to validate the docking protocol.

Table 1. The grid box used in the molecular dynamics studies.

| x-D | y-D | z-D | Spacing (Å) | x center | y center | z center |
|-----|-----|-----|-------------|----------|----------|----------|
| 40 | 40 | 40 | 0.581 | 165.852 | 145.231 | 189.106 |

A suitable gridbox was used to conduct molecular dynamics as shown in Table 1.

Following this, the molecular ligand library was computationally screened against the homology-modelled DNA-directed RNA polymerase of the monkeypox virus. The best lead molecule was identified based on a minimum binding energy of -5 to -15 kcal/mole [33, 38]. The binding scores of the ligand molecules with high affinity to the macromolecular target protein as well as the interacting residues and chemical structures were listed in Table 2. Analysis of the docking scores obtained after the computational screening of the designed library clearly showed that the α -amyrin had the strongest binding affinity towards the DNA-

directed RNA polymerase of the monkeypox virus.

3.3. Pharmacokinetic and Toxicological Evaluation

The characteristics of a drug molecule, such as its physicochemical and pharmacokinetic properties, are essential for the evaluation of its pharmacodynamics and toxicological qualities. Lipinski's rule of five

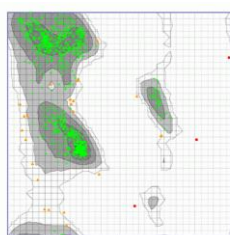


Figure 1. Ramachandran plot for the structural model of DNA-directed RNA polymerase of monkeypox virus.

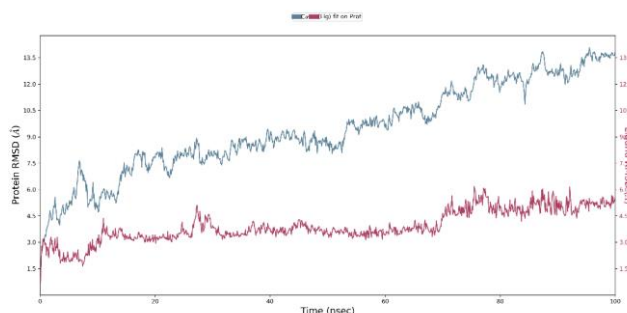


Figure 2. RMSD profiles of the $C\alpha$ backbone of DNA-directed RNA polymerase of monkeypox virus and α -amyrin observed during the MD simulation for 100 ns.

states that these parameters should be within a certain range, such as a molecular weight of less than 500, fewer than 10 hydrogen bond acceptors, fewer than 5 hydrogen bond donors, and a topological polar surface area of 20-130 Å², with the exception of the partition coefficient (LogP) value, which should be less than 0.5. The reported features of α -amyrin indicate that it has drug-like properties with improved pharmacokinetics. Additionally, P-glycoprotein serves as a natural filter for drugs, toxins, and other foreign substances. α -amyrin has not been predicted to act as a substrate for the P-glycoprotein, however, was predicted to act as a P-glycoprotein inhibitor. Similarly, α -amyrin was predicted not to act as CYP450 isoenzymes substrate, except CYP3A4. AMES, hERG-I inhibition, minnow toxicities were also investigated in the current study. Overall, based on physicochemical criteria, the projected pharmacokinetics and toxicological profile of α -amyrin matched well within the stated range, indicating that the molecule may be a good future therapeutic candidate [37, 43]. Table 3 lists the pharmacokinetic and toxicological features of shortlisted compounds.

3.4. Molecular Dynamics Simulation

MD simulation using the Schrodinger Desmond program was conducted to confirm the long-term stability of the DNA-directed RNA polymerase of the monkeypox virus when it was associated with the proposed herbal-based inhibitor molecule, α -amyrin. The macromolecular target has 1155 amino acid residues having 9317 heavy atoms out of total 18702 atoms and the ligand is having 31 heavy atoms out of total 81 atoms with only 1 rotatable bond. The protein backbone's stability and changes in structure were monitored by calculating the RMSD over the simulation period. Results from the MD simulation of the macromolecular target and α -amyrin complex showed that it remained stable throughout the 100 ns simulation, with an average RMSD value of between 5.0-13.5 Å for the macromolecular backbone. Despite some initial fluctuations for adjusting the ligand within the enzyme's cavity, the RMSD value of the ligand molecule was maintained within the 3-5 Å range throughout the simulation run. After attaining the active binding site of the DNA-directed RNA polymerase of the monkey-pox virus, the ligand α -amyrin went through a series of vibrations to attain the most consistent affirmation within the active binding site. Figure 2 displayed that RMSD profiles of the complex, ligand, and macromolecule had only slight variations and were consistent over time.

Table 2. The binding score achieved for each ligand from the intended ligand library against the monkeypox virus's DNA-directed RNA polymerase with the identified interaction residues.

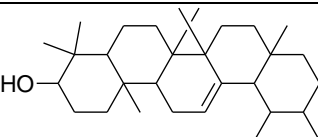
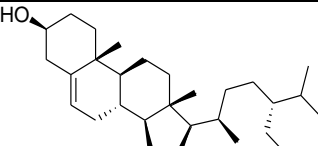
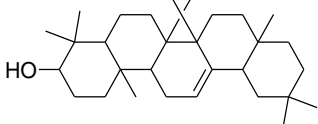
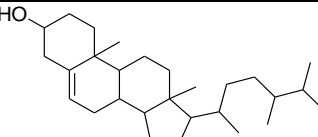
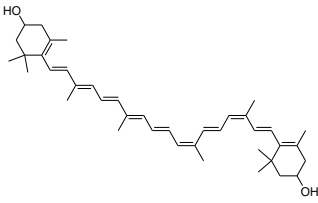
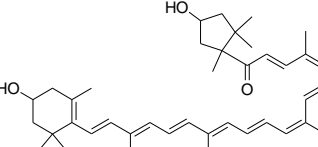
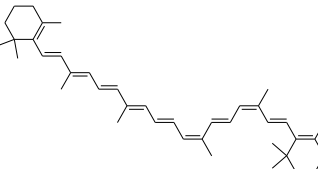
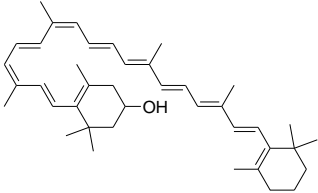
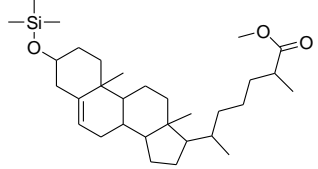
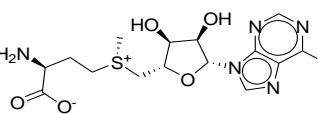
| Name | Structure | BE | Interacting Residues |
|-------------------------------|---|-------|--|
| α -amyrin |  | -8.19 | Arg45, Pro198, Val195, Ile174, Tyr205, Lys173, Lys421, Leu360, Glu172, Lys364, Tyr447 |
| β -sitosterol |  | -7.77 | His371, Ile49, Leu201, Tyr205, Val195, Glu172, Lys421, Thr368, Ile174, Lys173, Asp423, Tyr447, Lys364, Leu360 |
| β -amyrin |  | -7.71 | Pro198, Ser196, Val195, Tyr205, Ile174, Lys421, Tyr447, Lys173, Leu360, Glu172, Lys364 |
| Ergost-5-en-3-ol |  | -7.18 | Leu360, Lys421, Glu172, Thr368, Glu367, Arg45, Thr203, Val195, His207, His371, Tyr205, Ile174, Lys173 |
| Zeaxanthin |  | -6.79 | Arg45, His207, Lys364, Lys209, Ser224, Thr225, Thr175, Lys173, Ile174, Lys421, Ser193, Leu360, Tyr205, Glu367, Thr368 |
| Capsanthin |  | -6.77 | Lys364, Lys421, Lys173, Asp449, Val451, Lys179, His207, Lys420, Tyr205, Ile174, Val195, Thr368 |
| β -carotene |  | -6.61 | Val451, Asp449, Lys452, Glu367, His371, Thr203, Lys364, Val195, Thr368, Glu172, Leu360, Ile174, Tyr205, Lys421, Lys420, Glu450, Lys173 |
| β -cryptoxanthin |  | -6.52 | Ile174, Lys209, Tyr208, Ser191, Ser224, Thr225, His207, Lys226, Tyr205, Lys421, Lys173 |
| Methyl-3-hydroxycholestenoate |  | -6.40 | Arg206, Thr225, Tyr208, Lys209, Ser223, His207, Tyr205, His371, Arg204, Asn314 |
| SAM |  | -4.97 | Lys226, Thr227, His207, Tyr205, Thr225, Lys209, Gln8 |

Table 3. Physicochemical, pharmacokinetics, and pharmacodynamics properties of the lead molecules (Y= Yes; N=No).

| Property | Descriptor | α - amyirin | β - sitosterol | β -amyirin | Ergost- 5-en-3-ol | Zeaxanthin | Capsanthin | β -carotene | β -cryptoxanthin | Methyl-3- hydroxycholestenoate | SAM |
|----------------|---|-----------------------|-------------------------|------------------|----------------------|------------|------------|-------------------|------------------------|-----------------------------------|---------|
| MW | (g/mol) | 426.73 | 414.718 | 426.73 | 400.691 | 568.886 | 584.885 | 536.888 | 552.887 | 502.856 | 398.445 |
| LogP | - | 8.0248 | 8.0248 | 8.1689 | 7.6347 | 10.5474 | 9.8063 | 12.6058 | 11.5766 | 8.401 | -3.257 |
| Rotatable bond | - | 0 | 6 | 0 | 5 | 10 | 11 | 10 | 10 | 8 | 7 |
| HBA | - | 1 | 1 | 1 | 1 | 2 | 3 | 0 | 1 | 3 | 11 |
| HBD | - | 1 | 1 | 1 | 1 | 2 | 2 | 0 | 1 | 0 | 4 |
| TPSA | (Å) ² | 192.398 | 187.039 | 192.398 | 180.674 | 256.963 | 261.814 | 247.375 | 252.169 | 216.868 | 152.263 |
| Absorption | Water solubility (mol/L) | -6.906 | -6.871 | -7.001 | -7.006 | -6.903 | -6.968 | -7.314 | -7.17 | -7.146 | -2.685 |
| Absorption | CaCO ₂ permeability | 1.358 | 1.205 | 1.368 | 1.217 | 1.3 | 1.275 | 1.256 | 1.324 | 1.249 | -0.229 |
| Absorption | Intestinal absorption (%) (human) | 97.891 | 94.866 | 97.983 | 94.367 | 88.683 | 89.827 | 91.072 | 89.891 | 96.645 | 14.993 |
| Absorption | Skin Permeability (Log Kp) | -2.828 | -2.794 | -2.841 | -2.846 | -2.75 | -2.771 | -2.74 | -2.738 | -2.903 | -2.735 |
| Absorption | P-glycoprotein substrate | N | N | N | N | N | N | N | N | N | Y |
| Absorption | P-glycoprotein I inhibitor | Y | N | Y | N | N | N | N | N | Y | N |
| Absorption | P-glycoprotein II inhibitor | Y | Y | Y | Y | Y | Y | Y | Y | Y | N |
| Distribution | VDss (human) | 0.321 | 0.24 | 0.360 | 0.389 | -0.263 | -0.314 | 0.229 | -0.06 | 0.09 | -0.358 |
| Distribution | Fraction unbound (human) | 0 | 0 | 0 | 0 | 0 | 0 | 0 | 0 | 0 | 0.551 |
| Distribution | BBB permeability | 0.713 | 0.797 | 0.719 | 0.774 | -0.244 | -0.276 | 0.936 | 0.771 | -0.086 | -1.341 |
| Distribution | CNS permeability | -1.925 | -1.754 | -1.925 | -1.765 | -1.559 | -1.35 | -1.094 | -1.292 | -2.451 | -3.921 |
| Metabolism | CYP2D6 substrate | N | N | N | N | N | N | N | N | N | Y |
| Metabolism | CYP3A4 substrate | Y | Y | Y | Y | Y | Y | Y | Y | Y | N |
| Metabolism | CYP1A2 inhibitor | N | N | N | N | N | N | N | N | N | N |
| Metabolism | CYP2C19 inhibitor | N | N | N | N | N | N | N | N | N | N |

| | | | | | | | | | | | |
|------------|---|--------|--------|--------|--------|--------|--------|--------|--------|--------|-------|
| Metabolism | CYP2C9 inhibitor | N | N | N | N | N | N | N | N | N | N |
| Metabolism | CYP2D6 inhibitor | N | N | N | N | N | N | N | N | N | N |
| Metabolism | CYP3A4 inhibitor | N | N | N | N | N | N | N | N | N | N |
| Excretion | Total Clearance (log ml/min/kg) | 0.119 | 0.628 | -0.044 | 0.572 | 1.039 | 0.868 | 1.061 | 0.923 | 0.378 | 0.491 |
| Excretion | Renal OCT2 substrate | N | N | N | N | N | N | N | N | N | N |
| Toxicity | AMES toxicity | N | N | N | N | N | N | Y | N | N | N |
| Toxicity | Max. tolerated dose (human) (log mg/kg/day) | -0.275 | -0.555 | -0.086 | -0.525 | -1.143 | -1.152 | -0.423 | -0.845 | -0.452 | 0.643 |
| Toxicity | hERG I inhibitor | N | N | N | N | N | N | N | N | N | N |
| Toxicity | hERG II inhibitor | Y | Y | Y | Y | Y | N | Y | Y | N | N |
| Toxicity | Oral Rat Acute Toxicity (LD50) (mol/kg) | 2.345 | 2.326 | 2.333 | 2.173 | 2.629 | 2.552 | 2.111 | 2.468 | 2.49 | 2.416 |
| Toxicity | Oral Rat Chronic Toxicity (LOAEL) (mg/kg/day) | 1.031 | 0.829 | 1.041 | 0.876 | 2.596 | 2.402 | 0.64 | 0.658 | 1.954 | 2.291 |
| Toxicity | Hepatotoxicity | N | N | N | N | N | N | N | N | N | N |
| Toxicity | Skin Sensitization | N | N | N | N | N | N | N | N | N | N |
| Toxicity | <i>T. pyriformis</i> toxicity (mg/L) | 0.418 | 0.454 | 0.427 | 0.598 | 0.331 | 0.345 | 0.322 | 0.331 | 0.463 | 0.285 |
| Toxicity | MinNw toxicity | -1.953 | -2.12 | -2.074 | -1.888 | -2.722 | -2.523 | -3.899 | -3.25 | -2.759 | 2.354 |

The movement of amino acids in the active site was evaluated by calculating the RMSF of the macromolecule's $C\alpha$ atoms. This was done to identify the fluctuations of the amino acids in relation to their initial positions. The RMSF values of the residues are displayed on the y-axis of the RMSF plot, while their number is shown on the x-axis. Most of the residues of the macromolecular backbone, except the terminal ones, had RMSF values that ranged between 2 and 5 Å. It became evident that the fluctuations of the active amino acids had a mean variation of 2.0-2.5 Å, which is an acceptable range within the macromolecular active site. The MD simulation of 100 ns produced an RMSF plot for the $C\alpha$ backbones of the receptor macromolecule and ligand, as shown in Figure 3.

DNA-directed RNA polymerase of the monkeypox virus was analyzed throughout the MD simulation process and it was found that ligand molecule interacts with Ile174, Leu360, and Pro198 amino acid residues of the protein by hydrophobic interaction, amino acid Ser196 via forming a hydrogen bond, and amino acids Arg45, Pro197, Val200, Thr203, and Glu367 via forming water bridges. The interactions observed between the α -myrin and macromolecular target DNA-directed RNA polymerase of the monkeypox virus were demonstrated in residues throughout the simulation were demonstrated in Figure 5. The macromolecular target protein was found to be interacting with α -myrin through the residues such as Arg45, Pro197, Val200, Thr203, and

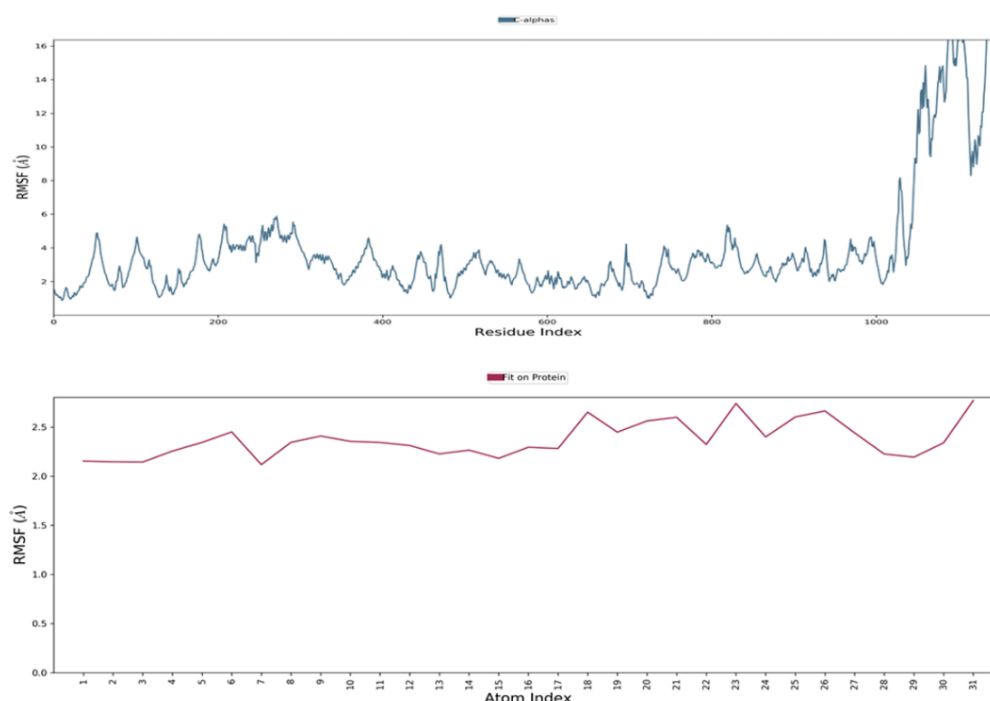


Figure 3. RMSF profiles of the DNA-directed RNA polymerase of monkeypox virus and α -myrin observed after performing the MD simulation for 100 ns.

Macromolecular secondary structures (α -helices (21.80%) and β -sheets (19.30%)) with a total of 41.10% were conserved throughout the simulation process. The stability of the receptor-ligand complex was due to the formation of hydrogen bonds, hydrophobic contacts, and ionic interactions throughout the MD simulation. To measure the stability of α -myrin, the intensity of these interactions was observed during MD simulation.

To measure the stability of α -myrin, the intensity of these interactions was observed during MD simulation. The interaction of α -myrin against the

Glu367 via water bridges, with residues Ile174 and Leu360 via hydrophobic interaction, and with Ser196 via classical hydrogen bonding with the ligand (Figure 5).

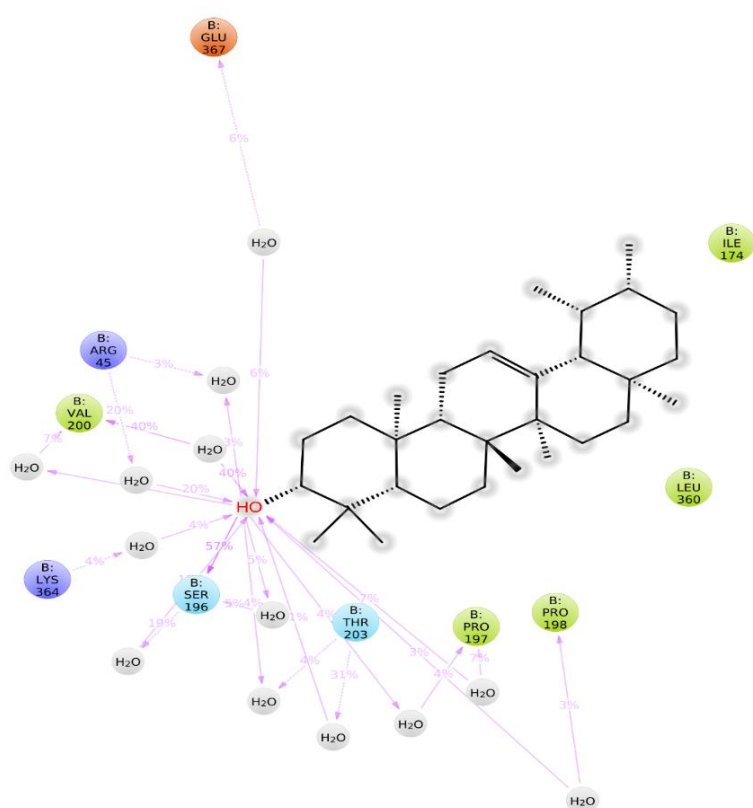


Figure 4. Analysis of the way α -amyryn interacts with viral DNA-directed RNA polymerase indicated that the macromolecular residues shown in green had hydrophobic connections, and the sky blue residues had polar connections with the complexed ligand. The orange-colored residues were negative, and the dark blue were positive.

4. Discussion

Monkeypox disease have been a public health concern in the history and humankind has occasionally faced monkeypox outbreaks [44, 45]. It is because of a smallpox-like virus, monkeypox virus, which can be transmitted via large respiratory droplets, close or direct contact with skin lesions, sexual intercourse, and possibly via contaminated fomites [46]. The most recent outbreak was declared as a global health emergency as of 24th of July, 2022. The number of monkeypox cases has been increasing around the globe and reached to around 31,000 within just three months. This number increased to more than 90,000 cases.

However, there is no currently available approved drugs specifically for monkeypox disease [17]. It is therefore urgent and essential to discover and develop novel drug candidate/s against monkeypox virus. It can also be beneficial to identify potential dietary supplement candidate/s as an alternative and easy-to-access option for the treatment of monkeypox disease, particularly in the poor regions of the world.

For the discovery of potential drug and/or dietary supplement candidate/s, this study focused on chili pepper as a medicinal plant. Chili pepper have used in the traditional medicine for the treatment of various diseases. For instance, Mayas used it for treating asthma, coughs, and sore, while the Aztecs used it to relieve toothaches [47]. In modern time, it is used in tear gas to control crowds by security agencies and has a wide range of application areas starting from culinary to pharmaceutical industry [48]. Various biological activities of chili pepper were summarized in the literature and can be listed as antioxidant, anticancer, anti-inflammatory, antiviral, antifungal, antiobesity, and antiplatelet [48–50]. Particularly for antiviral activities, chili extracts and one of the important natural products in chili pepper, capsaicin, showed promising antiviral activities against some viral species including herpes simplex virus, Lassa virus, and SARS-CoV-2 [24–27], indicating its antiviral potential for other viral species. In this study, we explored the antiviral potential of chili pepper against monkeypox virus using *in silico* techniques.

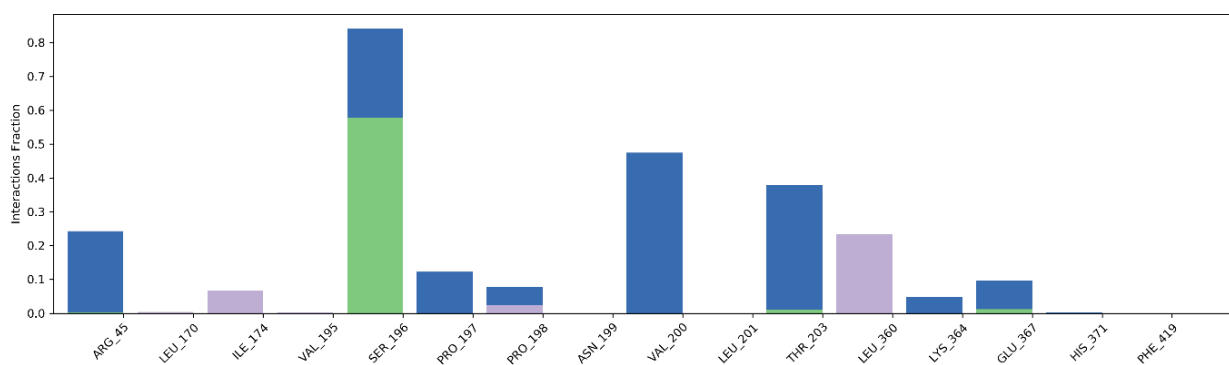


Figure 5. Protein-ligand contacts between viral RNA polymerase and complexed ligand α -amyrin. The green bars indicate H-bonds, the blue bars signify water bridges, the purple bars show hydrophobic interactions, and the dark pink bars highlight ionic interactions between the viral RNA polymerase and its complexed ligand, α -amyrin.

The molecular docking experiments in this study revealed that some of the natural products from chili pepper had strong binding affinities to the DNA-directed RNA polymerase of the monkeypox virus. The top lead molecules out of 47 ligands were tabulated in Table 2. Particularly, α -amyrin, β -sitosterol, and β -amyrin possess very low binding energy scores of -8.19, -7.77, and -7.71, respectively. Out of these hit molecules, MD simulations were conducted for α -amyrin complexed with the macromolecular target protein since it had the lowest binding energy value. Throughout the 100 ns MD simulation, α -amyrin complexed with DNA-directed RNA polymerase of the monkeypox virus was highly stable and it was interacting with some of the amino acid residues as shown in Figure 4. The structural similarity of these three lead compounds, which are pentacyclic triterpenes, might generate the expectation of having a similar profile in MD simulations for the other two lead compounds. In a recent study, Alandijany et al. also investigated potential drug candidates for monkeypox using DNA-directed RNA polymerase as well as viral core cysteine proteinase of monkeypox virus. They computationally discovered some of the tetracycline family ligands, exhibiting multi-target inhibition as a therapeutic solution for monkeypox viral infection [51]. While this study revealed that tetracyclic compounds can be potent against multi-target of monkeypox virus, our study indicated pentacyclic compounds can provide a potential solution for monkeypox outbreak. Furthermore, Akash et al. computationally investigated natural curcumin derivatives for the anti-viral drug discovery against monkeypox and smallpox infections and found that curcumin derivatives can indeed show potential for

the treatment of monkeypox and smallpox viruses with strong binding affinity toward profilin-like protein from monkeypox virus [52]. Interestingly, similar to our study and the study by Alandijany et al., curcumin derivatives with strong binding affinities indeed had multi-cyclic structures with three aromatic rings. This can unearth that multi-cyclic ligands can be potent antiviral agents in the prevention and treatment of monkeypox virus.

The pentacyclic triterpenes may be classified under four groups: oleanane, ursane, lupane and hopane. α -amyrin has an ursane skeleton, while β -amyrin has an oleanane skeleton. Amyrins are widely distributed in nature and exist in various plants and plant materials including leaves, bark, wood, and resins [53]. They exhibit various biological activities such as analgesic, anti-inflammatory, anxiolytic, anticonvulsant, anti-colitis, antidepressant, antihyperglycemic, anti-pancreatitis, and gastroprotective and hepatoprotective activities [53–55]. On the other hand, β -sitosterol is the main phytosterol found in the majority of plants and was reported to exhibit anti-inflammatory, antineoplastic, antipyretic, and immunomodulation activities [56]. However, there is not much literature showing the antiviral potential of amyryns. Glycyrrhetic acid, a derivative of the β -amyrin, was obtained from the herb liquorice and had an inhibitory effect on various viruses including hepatitis B virus (HBV) and HIV [57]. There is also some *in silico* studies for the antiviral potential of amyryns against SARS-CoV-2. For instance, α -amyrin and β -sitosterol were listed among the top-ranked molecules with the lowest binding energies towards both the spike glycoprotein of SARS-CoV-2 and human ACE2 receptor [58]. α - and β -amyrin were

also tested against main protease of SARS-CoV-2 using *in silico* approaches and showed strong binding affinities to the main protease [59]. To our knowledge, there is no study in the current literature showing the potential of amyryns as an antiviral agent against monkeypox virus. Thus, our study paved the way for the potential of amyryns as antiviral drug and/or dietary supplement candidate/s in the treatment of monkeypox disease.

5. Conclusion

In conclusion, due to the current outbreak of the monkeypox virus and the unavailability of approved drugs, there is an urgent need for the discovery and development of drug candidates effective against the monkeypox virus. In the current study, the natural products from chili pepper were evaluated for their potential antiviral activities against the monkeypox virus through *in silico* studies. The molecular docking experiments for 47 ligand molecules from chili pepper were performed against the homology-modeled DNA-directed RNA polymerase of the monkeypox virus. α -amyryn, β -sitosterol, and β -amyryn were among the top-ranked molecules with strong binding affinities towards DNA-directed RNA polymerase of the virus. In particular, the stability of

α -amyryn complexed with the macromolecular target was also confirmed with MD simulations. Because there is no study indicating the antiviral potential of α -amyryn against the monkeypox virus, this study revealed that α -amyryn has a potential inhibitory effect on DNA-directed RNA polymerase and could therefore constitute a potential lead molecule for the design of new antiviral agents against monkeypox. It also establishes α -amyryn as a possible dietary supplement candidate for monkeypox patients because it is a natural substance present in a variety of herbal and medicinal plants, including chili pepper.

Acknowledgement

No funding or financial aid have been received to support this research.

Conflict of Interest

The author declares no conflict of interest.

Statement of Research and Publication Ethics

This study complies with research and publication ethics

References

- [1] S. Riedel, "Edward Jenner and the history of smallpox and vaccination," *Proc. (Bayl. Univ. Med. Cent.)*, vol. 18, no. 1, p. 21, Jan. 2005, doi: 10.1080/08998280.2005.11928028.
- [2] J. Guarner, C. del Rio, and P. N. Malani, "Monkeypox in 2022—What Clinicians Need to Know," *JAMA*, vol. 328, no. 2, pp. 139–140, Jul. 2022, doi: 10.1001/JAMA.2022.10802.
- [3] S. R. Chowdhury, P. K. Datta, and S. Maitra, "Monkeypox and its pandemic potential: what the anaesthetist should know," *Br. J. Anaesth.*, vol. 0, no. 0, Jul. 2022, doi: 10.1016/J.BJA.2022.06.007.
- [4] E. M. Bunge *et al.*, "The changing epidemiology of human monkeypox—A potential threat? A systematic review," *PLoS Negl. Trop. Dis.*, vol. 16, no. 2, p. e0010141, Feb. 2022, doi: 10.1371/JOURNAL.PNTD.0010141.
- [5] Z. Ježek, M. Szczeniowski, K. M. Paluku, and M. Mutombo, "Human monkeypox: clinical features of 282 patients," *J Infect Dis*, vol. 156, pp. 293–298, 1987.
- [6] A. L. Hughes, S. Irausquin, and R. Friedman, "The evolutionary biology of poxviruses," *Infect. Genet. Evol.*, vol. 10, no. 1, pp. 50–59, Jan. 2010, doi: 10.1016/J.MEEGID.2009.10.001.
- [7] S. N. Shchelkunov *et al.*, "Human monkeypox and smallpox viruses: genomic comparison," *FEBS Lett.*, vol. 509, no. 1, pp. 66–70, Nov. 2001, doi: 10.1016/S0014-5793(01)03144-1.
- [8] C. T. Cho and H. A. Wenner, "Monkeypox Virus," *Bacteriol. Rev.*, vol. 37, no. 1, pp. 1–13, 1973, Accessed: Jul. 20, 2022. [Online]. Available: <https://journals.asm.org/journal/br>
- [9] F. S. Minhaj *et al.*, "Monkeypox Outbreak — Nine States, May 2022," *Morb. Mortal. Wkly. Rep.*, vol. 71, no. 23, p. 764, Jun. 2022, doi: 10.15585/MMWR.MM7123E1.
- [10] D. Mileto *et al.*, "New challenges in human monkeypox outside Africa: A review and case report from Italy," *Travel Med. Infect. Dis.*, vol. 49, p. 102386, Sep. 2022, doi: 10.1016/J.TMAID.2022.102386.

- [11] A. Zumla *et al.*, “Monkeypox outbreaks outside endemic regions: scientific and social priorities,” *Lancet Infect. Dis.*, vol. 22, no. 7, p. 929, Jul. 2022, doi: 10.1016/S1473-3099(22)00354-1.
- [12] D. W. Grosenbach *et al.*, “Oral Tecovirimat for the Treatment of Smallpox,” *N. Engl. J. Med.*, vol. 379, no. 1, pp. 44–53, Jul. 2018, doi: 10.1056/NEJMOA1705688.
- [13] G. Chittick, M. Morrison, T. Brundage, and W. G. Nichols, “Short-term clinical safety profile of brincidofovir: A favorable benefit–risk proposition in the treatment of smallpox,” *Antiviral Res.*, vol. 143, pp. 269–277, Jul. 2017, doi: 10.1016/j.antiviral.2017.01.009.
- [14] C. L. Hutson *et al.*, “Pharmacokinetics and efficacy of a potential smallpox therapeutic, brincidofovir, in a lethal monkeypox virus animal model,” *Am Soc Microbiol*, vol. 6, no. 1, Feb. 2022, doi: 10.1128/mSphere.00927-20.
- [15] A. T. Russo *et al.*, “Effects of treatment delay on efficacy of tecovirimat following lethal aerosol monkeypox virus challenge in cynomolgus macaques,” *J. Infect. Dis.*, vol. 218, no. 9, pp. 1490–1499, Sep. 2018, doi: 10.1093/INFDIS/JIY326.
- [16] H. Adler *et al.*, “Clinical features and management of human monkeypox: a retrospective observational study in the UK,” *Lancet Infect. Dis.*, vol. 22, no. 8, pp. 1153–1162, Aug. 2022, doi: 10.1016/S1473-3099(22)00228-6.
- [17] J. G. Rizk, G. Lippi, B. M. Henry, D. N. Forthal, and Y. Rizk, “Prevention and Treatment of Monkeypox.,” *Drugs*, vol. 82, no. 9, pp. 957–963, Jun. 2022, doi: 10.1007/S40265-022-01742-Y.
- [18] A. M. Vera-Guzmán, E. N. Aquino-Bolaños, E. Heredia-García, J. C. Carrillo-Rodríguez, S. Hernández-Delgado, and J. L. Chávez-Servia, “Flavonoid and Capsaicinoid Contents and Consumption of Mexican Chili Pepper (*Capsicum annuum* L.) Landraces,” *Flavonoids - From Biosynth. to Hum. Heal.*, Aug. 2017, doi: 10.5772/68076.
- [19] A. Wesołowska, D. J.-A. S. Pol., U. Hortorum, and U. 2011, “Chemical composition of the pepper fruit extracts of hot cultivars *Capsicum annuum* L.,” *Acta Sci. Pol., Hortorum Cultus*, vol. 10, no. 1, pp. 171–184, 2011, Accessed: Jul. 26, 2022. [Online]. Available: <https://czasopisma.up.lublin.pl/index.php/asphc/article/view/3190>.
- [20] S. E. Altmann *et al.*, “Inhibition of cowpox virus and monkeypox virus infection by mitoxantrone,” *Antiviral Res.*, vol. 93, no. 2, pp. 305–308, Feb. 2012, doi: 10.1016/J.ANTIVIRAL.2011.12.001.
- [21] J. Deval, J. A. Symons, and L. Beigelman, “Inhibition of viral RNA polymerases by nucleoside and nucleotide analogs: therapeutic applications against positive-strand RNA viruses beyond hepatitis C virus,” *Curr. Opin. Virol.*, vol. 9, p. 1, 2014, doi: 10.1016/J.COVIRO.2014.08.004.
- [22] S. Mujwar, L. Sun, and O. Fidan, “*In silico* evaluation of food-derived carotenoids against SARS-CoV-2 drug targets: Crocin is a promising dietary supplement candidate for COVID-19,” *J. Food Biochem.*, p. e14219, 2022, doi: 10.1111/JFBC.14219.
- [23] Y. Furuta, B. B. Gowen, K. Takahashi, K. Shiraki, D. F. Smee, and D. L. Barnard, “Favipiravir (T-705), a novel viral RNA polymerase inhibitor,” *Antiviral Res.*, vol. 100, no. 2, pp. 446–454, Nov. 2013, doi: 10.1016/J.ANTIVIRAL.2013.09.015.
- [24] N. Rahmattullah, E. Laras Arumingtyas, M. Hermawan Widyananda, A. N. Ahyar, and I. Tabroni, “Bioinformatics Analysis of Bioactive Compounds of Four *Capsicum* Species against SARS-CoV-2 Infection,” *Int. J. Adv. Biol. Biomed. Res.*, vol. 9, no. 4, pp. 298–319, 2021, doi: 10.22034/ijabbr.2021.139183.1335.
- [25] N. Ordaz-Trinidad, L. Dorantes-Álvarez, J. Salas-Benito, B. L. Barrón-Romero, M. Salas-Benito, and M. De Nova-Ocampo, “Cytotoxicity and antiviral activity of pepper extracts (*Capsicum* spp),” *Polibotánica*, vol. 0, no. 46, Jul. 2018, doi: 10.18387/POLIBOTANICA.46.18.
- [26] K. Tang, X. Zhang, and Y. Guo, “Identification of the dietary supplement capsaicin as an inhibitor of Lassa virus entry,” *Acta Pharm. Sin. B*, vol. 10, no. 5, pp. 789–798, May 2020, doi: 10.1016/J.APSB.2020.02.014.
- [27] T. A. Hafiz, M. A. Mubarak, M. A. Dkhil, and S. Al-Quraishy, “Antiviral Activities of *Capsicum annuum* Methanolic Extract against Herpes Simplex Virus 1 and 2,” *Pak. J. Zool.*, vol. 49, no. 1, pp. 251–255, Jan. 2017, doi: 10.17582/JOURNAL.PJZ/2017.49.1.251.255.
- [28] K. H. Choi, “Viral polymerases,” *Adv. Exp. Med. Biol.*, vol. 726, pp. 267–304, 2012, doi: 10.1007/978-1-4614-0980-9_12/COVER.

- [29] A. Bateman *et al.*, “UniProt: the universal protein knowledgebase in 2021,” *Nucleic Acids Res.*, vol. 49, no. D1, p. D480, Jan. 2021, doi: 10.1093/NAR/GKAA1100.
- [30] W. D. Arndt *et al.*, “Monkeypox virus induces the synthesis of less dsRNA than vaccinia virus, and is more resistant to the anti-poxvirus drug, IBT, than vaccinia virus,” *Virology*, vol. 497, pp. 125–135, Oct. 2016, doi: 10.1016/J.VIROL.2016.07.016.
- [31] A. Waterhouse *et al.*, “SWISS-MODEL: homology modelling of protein structures and complexes,” *Nucleic Acids Res.*, vol. 46, no. W1, pp. W296–W303, Jul. 2018, doi: 10.1093/NAR/GKY427.
- [32] K. Gopalakrishnan, G. Sowmiya, S. S. Sheik, and K. Sekar, “Ramachandran Plot on The Web (2.0),” *Protein Pept. Lett.*, vol. 14, no. 7, pp. 669–671, Aug. 2007, doi: 10.2174/092986607781483912.
- [33] S. Mujwar and R. K. Harwansh, “*In silico* bioprospecting of taraxerol as a main protease inhibitor of SARS-CoV-2 to develop therapy against COVID-19,” *Struct. Chem.*, vol. 1, p. 1, 2022, doi: 10.1007/S11224-022-01943-X.
- [34] O. Fidan, S. Mujwar, and M. Kciuk, “Discovery of adapalene and dihydrotachysterol as antiviral agents for the Omicron variant of SARS-CoV-2 through computational drug repurposing,” *Mol. Divers.*, vol. 27, no. 1, pp. 463–475, Feb. 2023, doi: 10.1007/S11030-022-10440-6.
- [35] S. Mujwar, K. Shah, J. K. Gupta, and A. Gour, “Docking based screening of curcumin derivatives: A novel approach in the inhibition of tubercular DHFR,” *Int. J. Comput. Biol. Drug Des.*, vol. 14, no. 4, pp. 297–314, 2021, doi: 10.1504/IJCBDD.2021.118830.
- [36] S. Mujwar, “Computational bioprospecting of andrographolide derivatives as potent cyclooxygenase-2 inhibitors,” *Biomed. Biotechnol. Res. J.*, vol. 5, no. 4, p. 446, Oct. 2021, doi: 10.4103/BBRJ.BBRJ_56_21.
- [37] D. E. V. Pires, T. L. Blundell, and D. B. Ascher, “pkCSM: Predicting small-molecule pharmacokinetic and toxicity properties using graph-based signatures,” *J. Med. Chem.*, vol. 58, no. 9, pp. 4066–4072, May 2015, doi: 10.1021/ACS.JMEDCHEM.5B00104.
- [38] R. Jain and S. Mujwar, “Repurposing metocurine as main protease inhibitor to develop novel antiviral therapy for COVID-19,” *Struct. Chem.*, pp. 1–13, 2020, doi: <https://doi.org/10.1007/s11224-020-01605-w>.
- [39] S. Mujwar, “Computational repurposing of tamibarotene against triple mutant variant of SARS-CoV-2,” *Comput Biol Med*, vol. 136, p. 104748, 2021, doi: <https://doi.org/10.1016/j.compbiomed.2021.104748>.
- [40] K. Shah, S. Mujwar, G. Krishna, and J. K. Gupta, “Computational Design and Biological Depiction of Novel Naproxen Derivative,” *<https://home.liebertpub.com/adt>*, vol. 18, no. 7, pp. 308–317, Oct. 2020, doi: 10.1089/ADT.2020.977.
- [41] H. S. Hillen *et al.*, “Structural Basis of Poxvirus Transcription: Transcribing and Capping Vaccinia Complexes,” *Cell*, vol. 179, no. 7, pp. 1525–1536.e12, Dec. 2019, doi: 10.1016/J.CELL.2019.11.023.
- [42] C. Grimm, J. Bartuli, B. Boettcher, A. A. Szalay, and U. Fischer, “Structural basis of the complete poxvirus transcription initiation process,” *Nat. Struct. Mol. Biol.* 2021 2810, vol. 28, no. 10, pp. 779–788, Sep. 2021, doi: 10.1038/s41594-021-00655-w.
- [43] L. Z. Benet, C. M. Hosey, O. Ursu, and T. I. Oprea, “BDDCS, the Rule of 5 and drugability,” *Adv. Drug Deliv. Rev.*, vol. 101, pp. 89–98, Jun. 2016, doi: 10.1016/J.ADDR.2016.05.007.
- [44] B. L. Ligon, “Monkeypox: A review of the history and emergence in the Western hemisphere,” *Semin. Pediatr. Infect. Dis.*, vol. 15, no. 4, pp. 280–287, Oct. 2004, doi: 10.1053/J.SPID.2004.09.001.
- [45] J. S. Bryer, E. E. Freeman, and M. Rosenbach, “Monkeypox emerges on a global scale: a historical review and dermatological primer,” *J. Am. Acad. Dermatol.*, Jul. 2022, doi: 10.1016/J.JAAD.2022.07.007.
- [46] J. P. Thornhill *et al.*, “Monkeypox Virus Infection in Humans across 16 Countries - April-June 2022.,” *N. Engl. J. Med.*, Jul. 2022, doi: 10.1056/NEJMOA2207323.
- [47] B. K. Saleh, “Medicinal uses and health benefits of chili pepper (*Capsicum* spp.): a review Evaluation of husbandry, insect pest, diseases and management practices of vegetables cultivated in Zoba Anseba Eritrea View project Mycology isolation of fungi from sorghum pearl millet View project,” 2018, doi: 10.15406/mojfpt.2018.06.00183.
- [48] S. Idrees, M. A. Hanif, M. A. Ayub, A. Hanif, and T. M. Ansari, “Chili Pepper,” *Med. Plants South Asia Nov. Sources Drug Discov.*, pp. 113–124, Jan. 2020, doi: 10.1016/B978-0-08-102659-5.00009-4.

- [49] G. E. S. Batiha *et al.*, “Biological Properties, Bioactive Constituents, and Pharmacokinetics of Some *Capsicum* spp. and Capsaicinoids,” *Int. J. Mol. Sci.*, vol. 21, no. 15, pp. 1–35, Aug. 2020, doi: 10.3390/IJMS21155179.
- [50] K. Srinivasan, “Biological Activities of Red Pepper (*Capsicum annuum*) and Its Pungent Principle Capsaicin: A Review,” <http://dx.doi.org/10.1080/10408398.2013.772090>, vol. 56, no. 9, pp. 1488–1500, Jul. 2015, doi: 10.1080/10408398.2013.772090.
- [51] T. A. Alandijany *et al.*, “A multi-targeted computational drug discovery approach for repurposing tetracyclines against monkeypox virus,” *Sci. Reports* 2023 131, vol. 13, no. 1, pp. 1–22, Sep. 2023, doi: 10.1038/s41598-023-41820-z.
- [52] S. Akash *et al.*, “Anti-viral drug discovery against monkeypox and smallpox infection by natural curcumin derivatives: A Computational drug design approach,” *Front. Cell. Infect. Microbiol.*, vol. 13, p. 1157627, 2023, doi: 10.3389/FCIMB.2023.1157627.
- [53] A. O. Nogueira, Y. I. S. Oliveira, B. L. Adjafre, M. E. A. de Moraes, and G. F. Aragão, “Pharmacological effects of the isomeric mixture of alpha and beta amyryn from *Protium heptaphyllum*: a literature review,” *Fundam. Clin. Pharmacol.*, vol. 33, no. 1, pp. 4–12, Feb. 2019, doi: 10.1111/FCP.12402.
- [54] F. A. Santos *et al.*, “Antihyperglycemic and hypolipidemic effects of α,β -amyryn, a triterpenoid mixture from *Protium heptaphyllum* in mice,” *Lipids Health Dis.*, vol. 11, no. 1, pp. 1–8, Aug. 2012, doi: 10.1186/1476-511X-11-98.
- [55] G. F. Aragao, M. C. C. Pinheiro, P. N. Bandeira, T. L. G. Lemos, and G. S. de B. Viana, “Analgesic and Anti-Inflammatory Activities of the Isomeric Mixture of Alpha- and Beta-Amyryn from *Protium heptaphyllum*(Aubl.) March,” http://dx.doi.org/10.1080/J157v07n02_03, vol. 7, no. 2, pp. 31–47, Jan. 2009, doi: 10.1080/J157V07N02_03.
- [56] L. Fraile, E. Crisci, L. Córdoba, M. A. Navarro, J. Osada, and M. Montoya, “Immunomodulatory properties of Beta-sitosterol in pig immune responses,” *Int. Immunopharmacol.*, vol. 13, no. 3, pp. 316–321, Jul. 2012, doi: 10.1016/J.INTIMP.2012.04.017.
- [57] R. Pompei, O. Flore, M. A. Marccialis, A. Pani, and B. Loddo, “Glycyrrhizic acid inhibits virus growth and inactivates virus particles,” *Nat.* 1979 2815733, vol. 281, no. 5733, pp. 689–690, 1979, doi: 10.1038/281689a0.
- [58] V. K. Maurya, S. Kumar, M. L. B. Bhatt, and S. K. Saxena, “Antiviral activity of traditional medicinal plants from Ayurveda against SARS-CoV-2 infection,” *J. Biomol. Struct. Dyn.*, vol. 40, no. 4, pp. 1719–1735, 2022, doi: 10.1080/07391102.2020.1832577.
- [59] B. Kar, B. Dehury, M. K. Singh, S. Pati, and D. Bhattacharya, “Identification of phytocompounds as newer antiviral drugs against COVID-19 through molecular docking and simulation based study,” *J. Mol. Graph. Model.*, vol. 114, p. 108192, Jul. 2022, doi: 10.1016/J.JMGM.2022.108192.